Supporting Information for:

Toward Tuning the Bandgap in Meta-Substituted Fe-MOFs – Supplemental Information

Kyle I. Williamson, Daniel J.C. Herr, Yirong Mo**

Department of Nanoscience, Joint School of Nanoscience and Nanoengineering, University of North Carolina at Greensboro, Greensboro, NC 27401, USA

Table of Contents

Section S1. Plotting the half normal for bandgap, HOMO, and LUMO.

The charts below are the half normal vs. standardized coefficients for bandgap, HOMO, and LUMO results from the Fe-MOF-5 models used in this study. Per the ECHIP manual, when the plotted points form a straight line in a half-normal plot, then the coefficient estimates contain only error. The general procedure is to draw a line passing through a substantial number of the smallest points, on the assumption that they are made up from error alone. Thus, you may interpret points not falling on this line as significant. Half-normal plotting is very effective when replicates have not been taken, because it allows you to use a line through the smallest points as an estimate of the replicate standard deviation. The estimate is the value on the vertical axis corresponding to the point where the line crosses unity on the half normal axis.[1]

We report this method to represent the lack of statistical significance in a graphical manner. While none of the response factors (bandgap, HOMO, or LUMO) have statistically significant coefficients/factors, the trend can still be informative. To model as closely as possible to the outputted response factors, we include the σ_m, ε, $\sigma_m * \varepsilon$, and $\sigma_m * \varepsilon^2$ terms. From these qualitative trends, we are able to surmise potential fundamental interactions between σ_m and ε that are discussed in the main article. A final consideration from these results is that the Fe-MOF-5 models are resistant to changes in electronic structure under modification of substituent groups and solvent alike. This aligns with previous research indicating the stability of Fe-MOFs in various environments.[2,3]

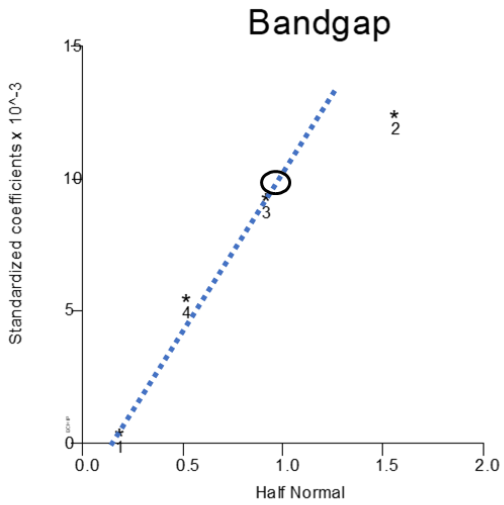

Figure S1. Half Normal plot of Bandgap, with the estimated replicate standard deviation using the method described previously being ~10*10^-3.

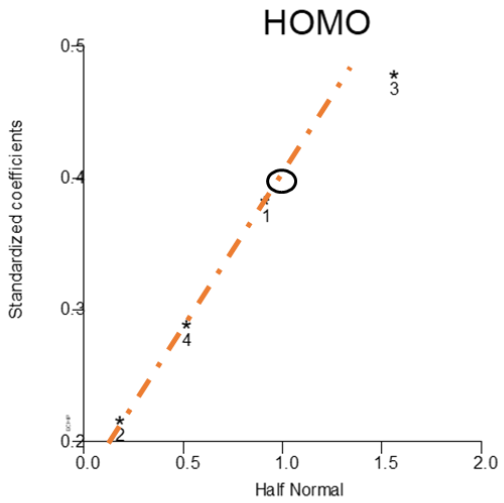

Figure S2. Half Normal plot of HOMO, with the estimated replicate standard deviation using the method described previously being 0.4.

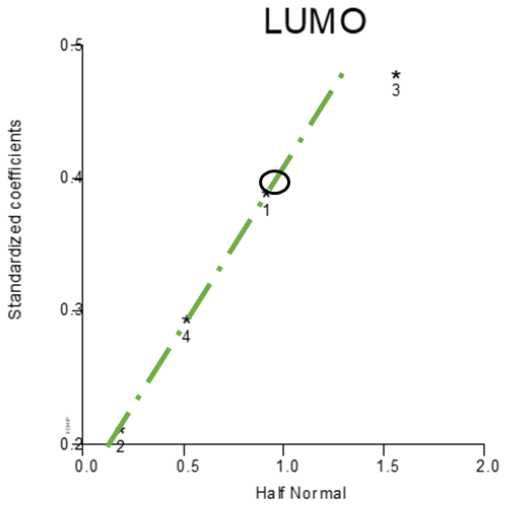

Figure S3. Half Normal plot of LUMO, with the estimated replicate standard deviation using the method described previously being 0.4.

Section S2. Supplemental Figures

Figure S4. Representative optimized models of Fe-MOF-5. As the implicit solvent seems to have no statistical impact, just like the substituent group, the models below represent the different configurations based on the substituent group.

Fe-MOF-5

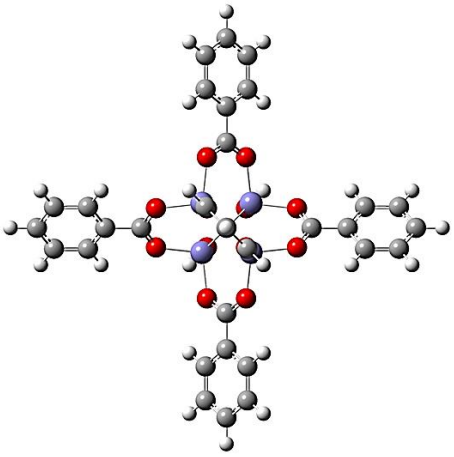

Fe-MOF-5 with NH_2

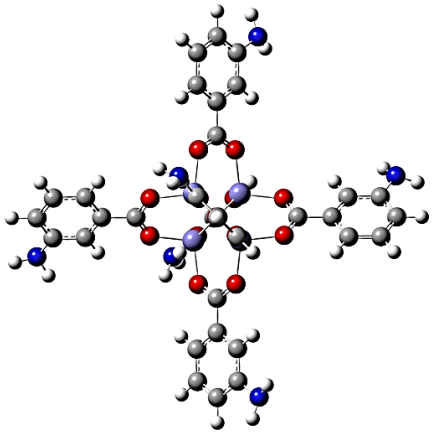

Fe-MOF-5 with CF_3

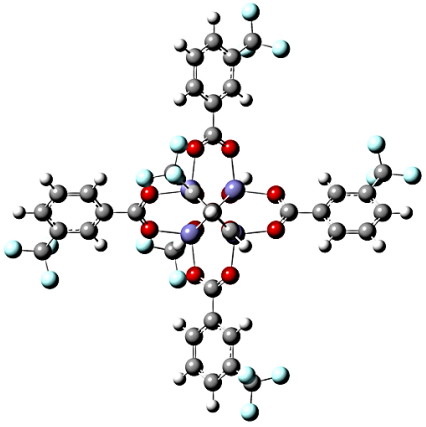

Fe-MOF-5 with NO_2

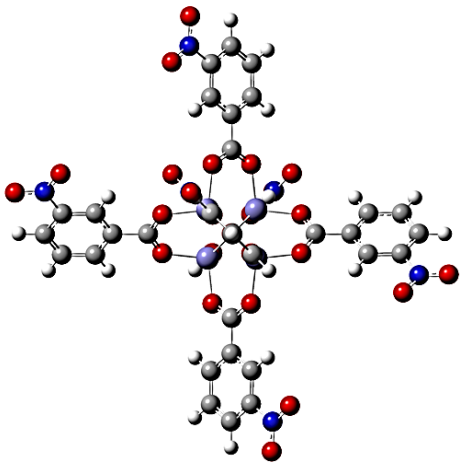

Fe-MOF-5 with CH_3

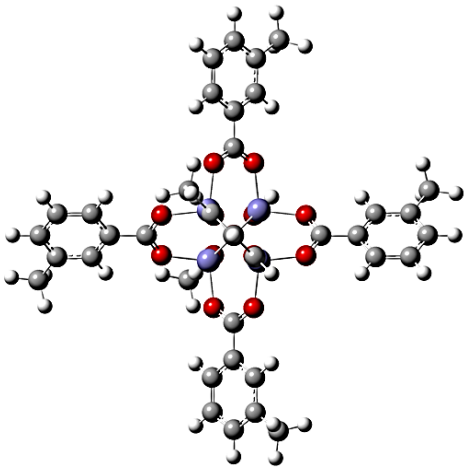

Fe-MOF-5 with CHO

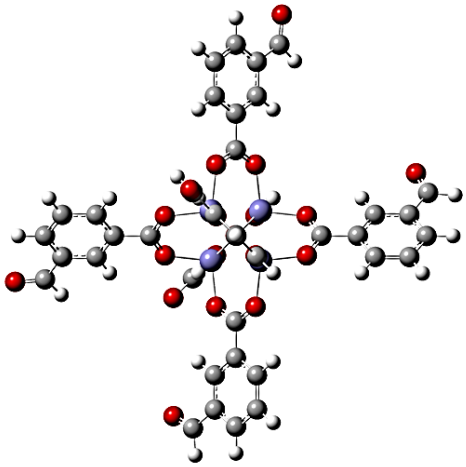

Fe-MOF-5 with NO

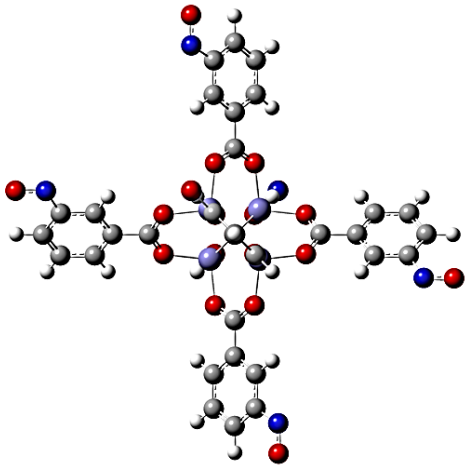

Fe-MOF-5 with CN

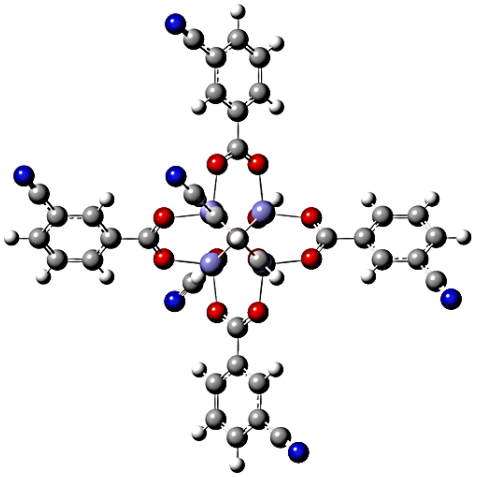

Fe-MOF-5 with SH

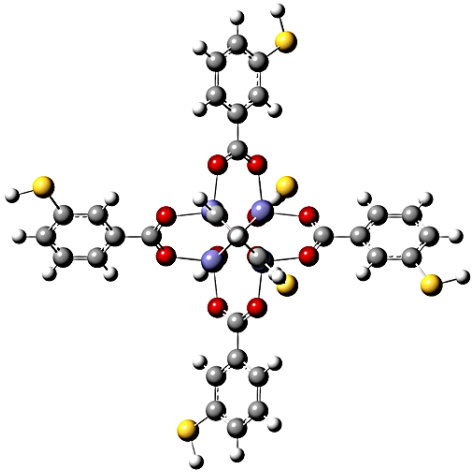

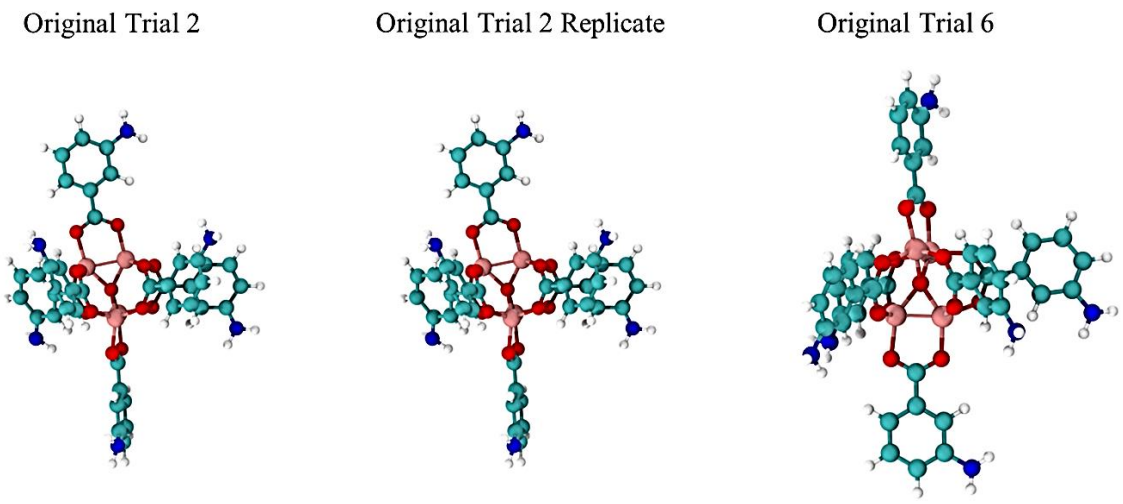

Figure S5. The unphysical optimized geometries of the original trial 2, trial 2 replicate, and trail 6. While each trial has NH as the substituent group, the metal nods (red and pink atoms) are heavily distorted, resulting in the whole structure twisting. As the expectation is that MOF-5 transmetalated with iron will maintain the same lattice as MOF-5, these three trials were taken out of the data set before analysis with EChip.

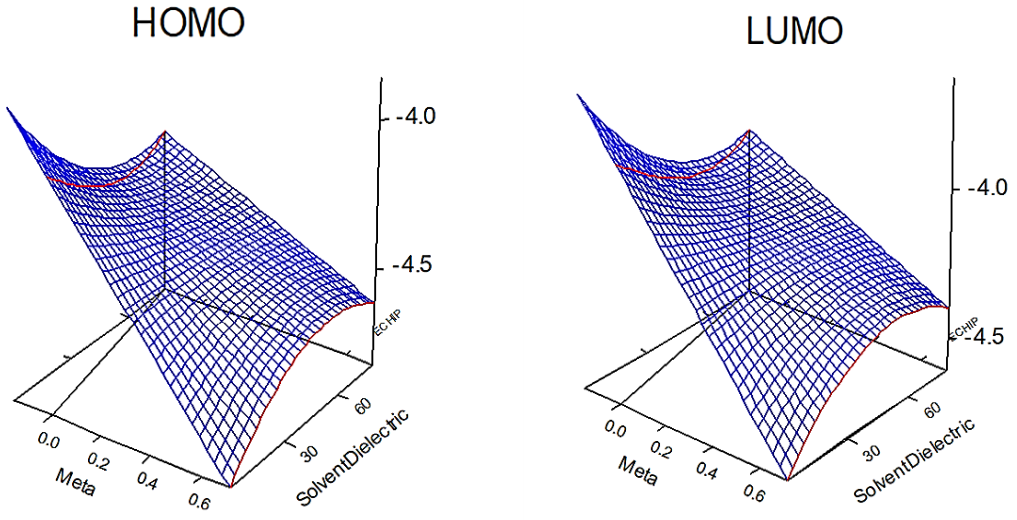

Figure S6. The 3D response surface of the HOMO and LUMO energy levels across the Fe-MOF-5 models. Note the red and black lines on the left side of each graph. These intersections with the surfaces indicate that anything plotted to the left of that line is an extrapolation and no conclusion should be drawn based on this portion of the surface.

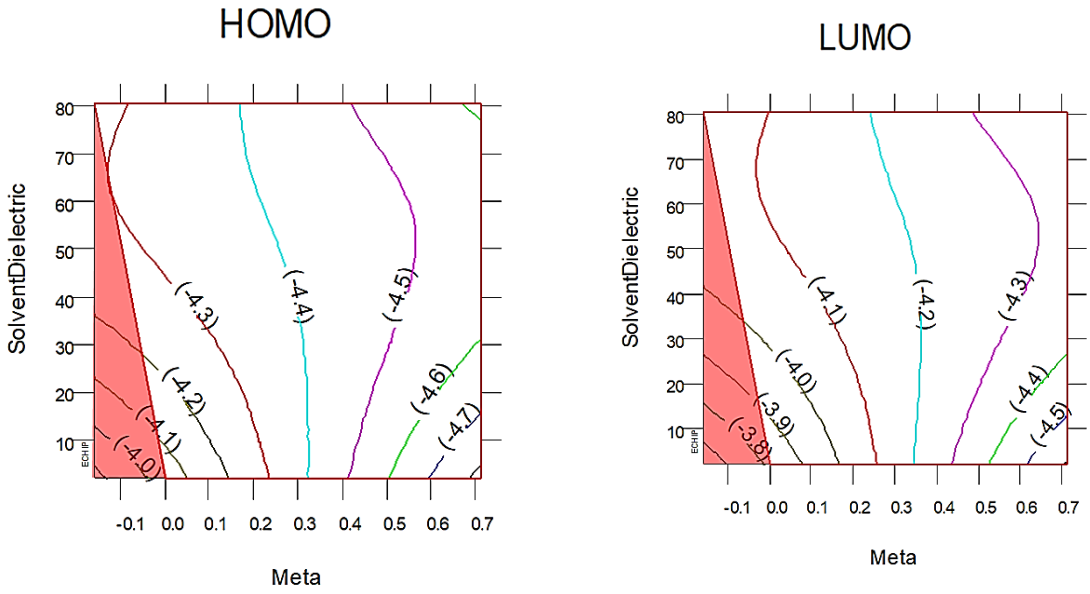

Figure S7. The 2D response surface of the HOMO and LUMO energy levels across the Fe-MOF-5 models. Note the red and black lines on the left side of each graph. These intersections with the surfaces indicate that anything plotted to the left of that line is an extrapolation and no conclusion should be drawn based on this portion of the surface. At lower solvent dielectric (ε) the meta (σ_m) term has a larger impact on HOMO and LUMO energy levels as shown with the closer spacing of the colored line. These colored lines represent 2σ significance. On the other hand, at higher ε values the σ_m term become less significant as the lines 2σ bulge out. This shift occurs around the same area where the ε term begins to dominate the bandgap as seen in Figure 3.

A. Density of States for Fe-MOF-5-CHO

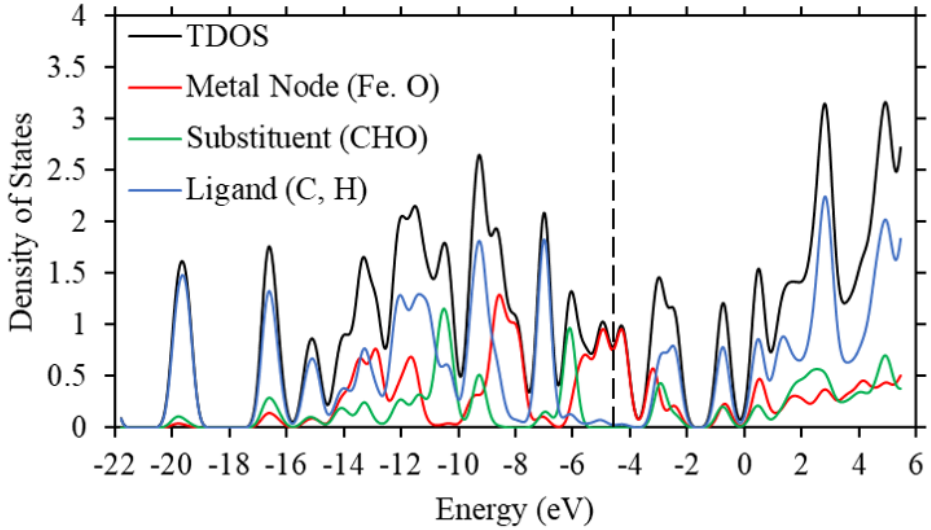

B. Discrete Energy Levels for Fe-MOF-5-CHO

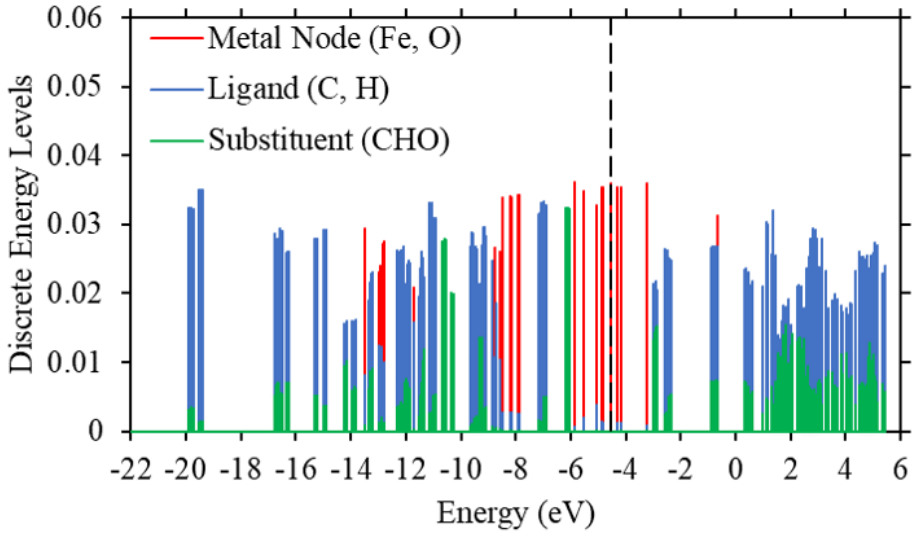

Figure S8. A. TDOS and PDOS maps of Fe-MOF-5-CHO (Trial 17) across the bandgap response surface at a ε value of 1.89 (Hexane). B. The discrete energy levels of the ligand (blue), the metal node (red), and the substituent (green). The vertical dashed line in both A and B represents the HOMO energy level of the Fe-MOF-5-CHO system, which is at -4.543 eV. The y-axis represents the strength of the density of states and discrete energy levels and are unitless.

A. Density of States for Fe-MOF-5-NO_2

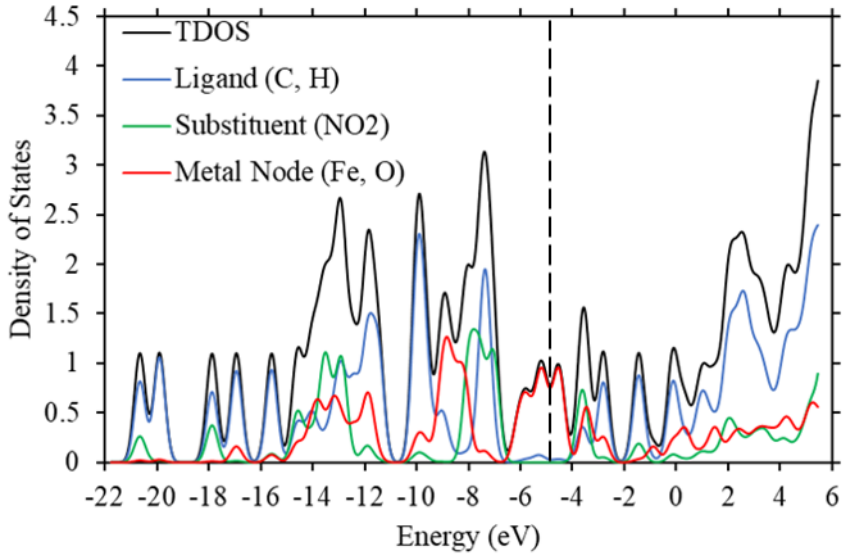

B. Discrete Energy Levels for Fe-MOF-5-NO_2

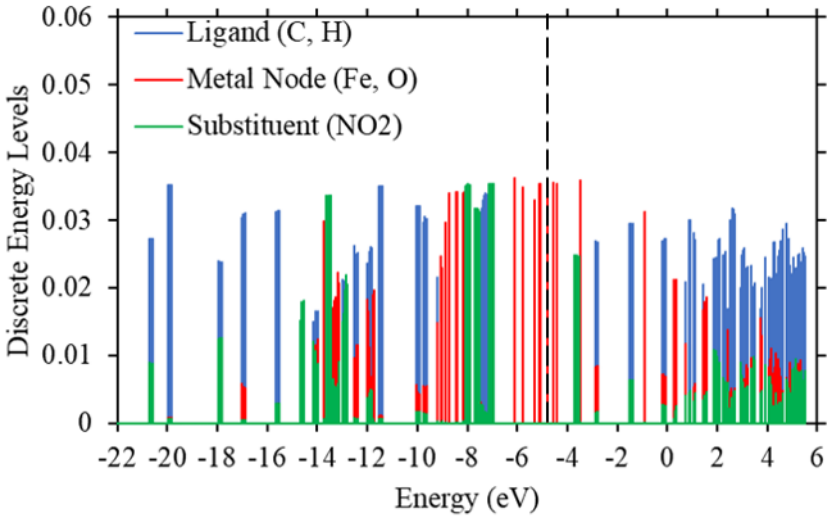

Figure S9. A. TDOS and PDOS maps of Fe-MOF-5-NO_2 (Trial 5) across the bandgap response surface at a ε value of 1.89 (Hexane). B. The discrete energy levels of the ligand (blue), the metal node (red), and the substituent (green). The vertical dashed line in both A and B represents the HOMO energy level of the Fe-MOF-5-NO_2 system, which is at -4.786 eV. The y-axis represents the strength of the density of states and discrete energy levels and are unitless.

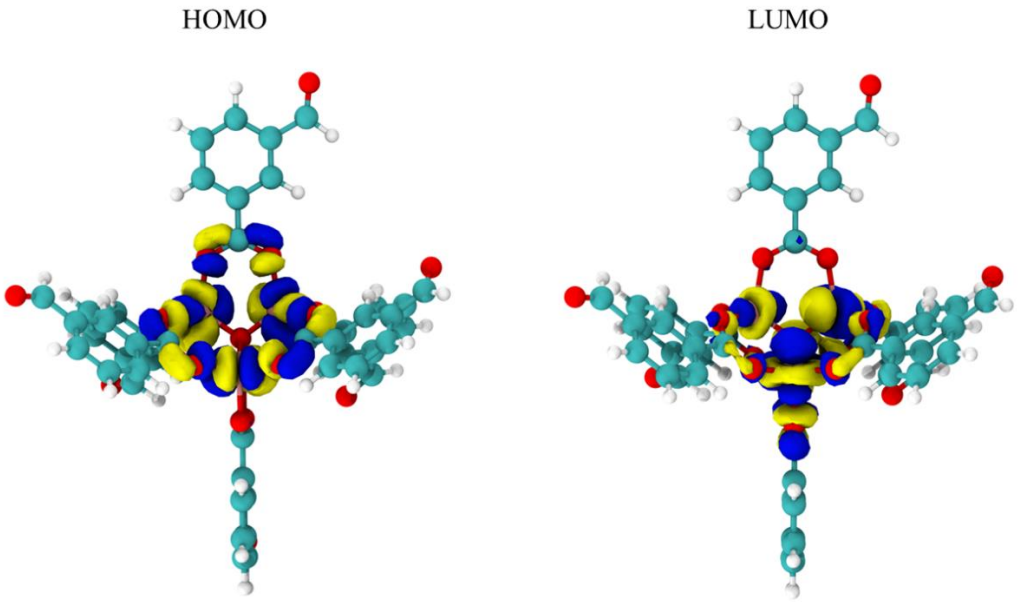

Figure S10. The HOMO and LUMO molecular orbitals of Fe-MOF-5-CHO (Trial 17). The positive orbital wave function is represented by the blue regions, while the negative orbital wave function is represented by the yellow regions. In both the HOMO and LUMO, the primary electron occupancy is around the metal node comprise of iron and oxygen atoms.

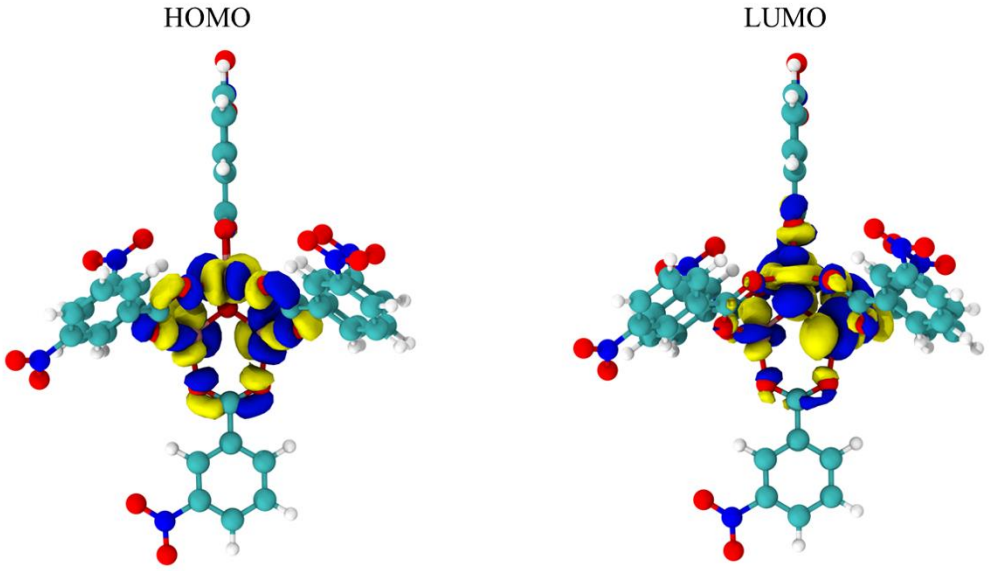

Figure S11. The HOMO and LUMO molecular orbitals of Fe-MOF-5-NO_2 (Trial 5). The positive orbital wave function is represented by the blue regions, while the negative orbital wave function is represented by the yellow regions. In both the HOMO and LUMO, the primary electron occupancy is around the metal node comprise of iron and oxygen atoms.

A. Density of States for Fe-MOF-5 (Hexane)

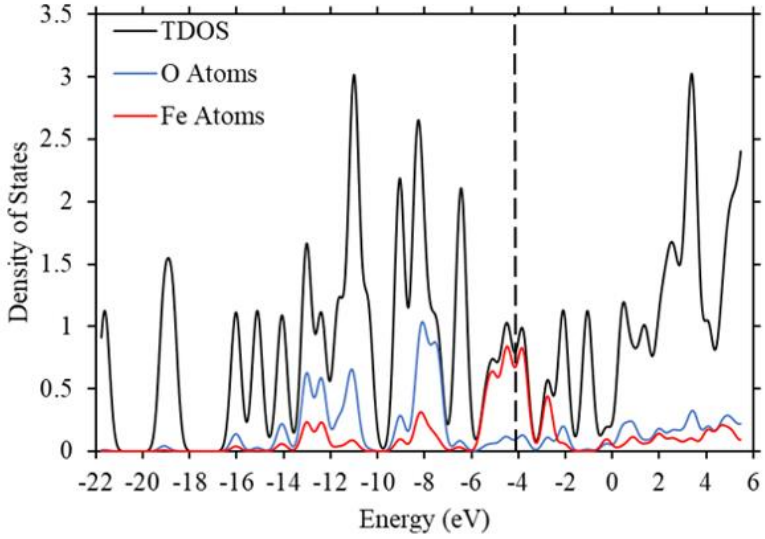

B. Discrete Energy Levels for Fe-MOF-5 (Hexane)

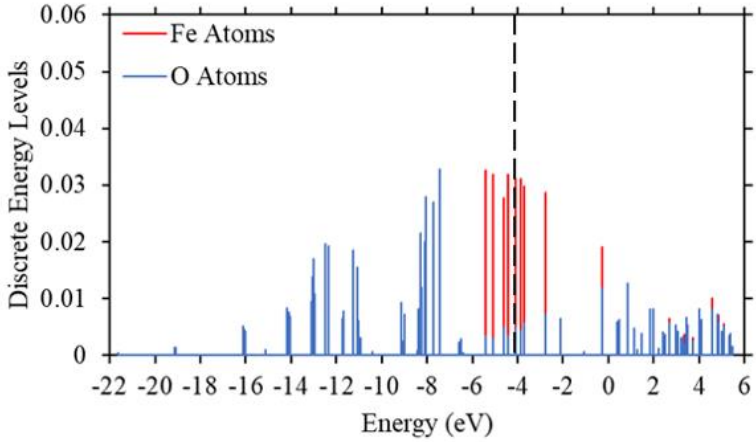

Figure S12. A. TDOS and PDOS graph of the contributions of the iron and oxygen in Fe-MOF-5 in hexane (Trial 20). B. The discrete energy levels of the oxygen atoms (blue) and the iron atoms (red). Light vertical dashed lines represent the HOMO energy level at -4.104 eV. The y-axis represents the strength of the density of states and discrete energy levels and are unitless.

A. Density of States for Fe-MOF-5-CHO (Hexane)

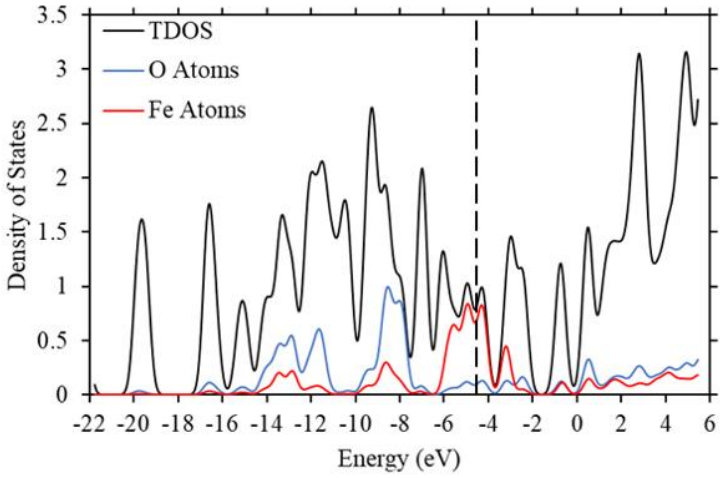

B. Discrete Energy Levels for Fe-MOF-5-CHO (Hexane)

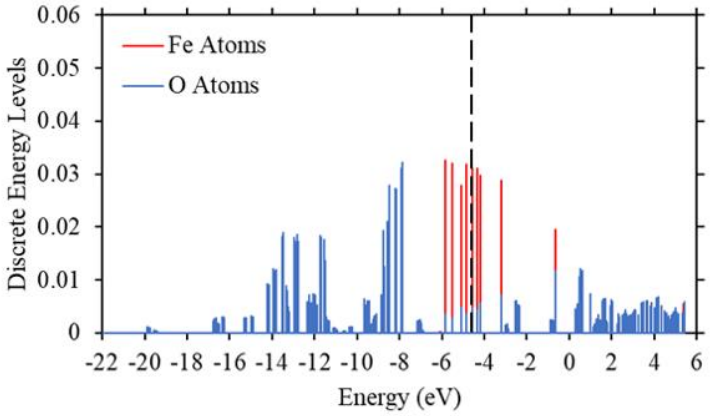

Figure S13. A. TDOS and PDOS graph of the contributions of the iron and oxygen in Fe-MOF-5-CHO in hexane (Trial 17). B. The discrete energy levels of the oxygen atoms (blue) and the iron atoms (red). The vertical dashed line in both A and B represents the HOMO energy level of the Fe-MOF-5-CHO system, which is at -4.543 eV. The y-axis represents the strength of the density of states and discrete energy levels and are unitless.

A. Density of States for Fe-MOF-5-NO_2 (Hexane)

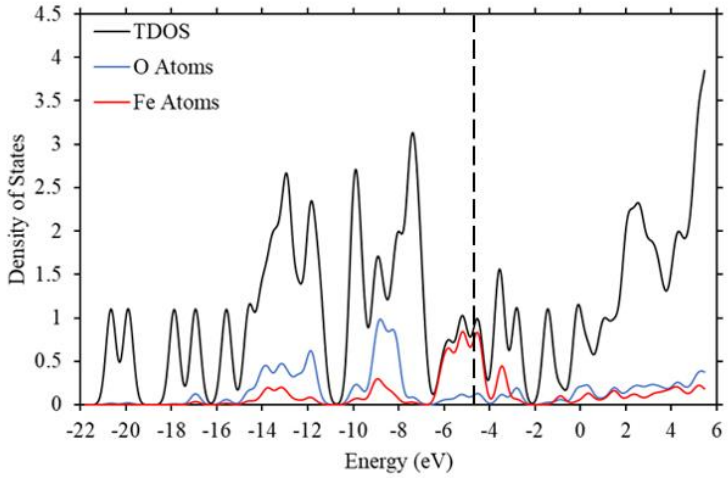

B. Discrete Energy Levels for Fe-MOF-5-NO_2 (Hexane)

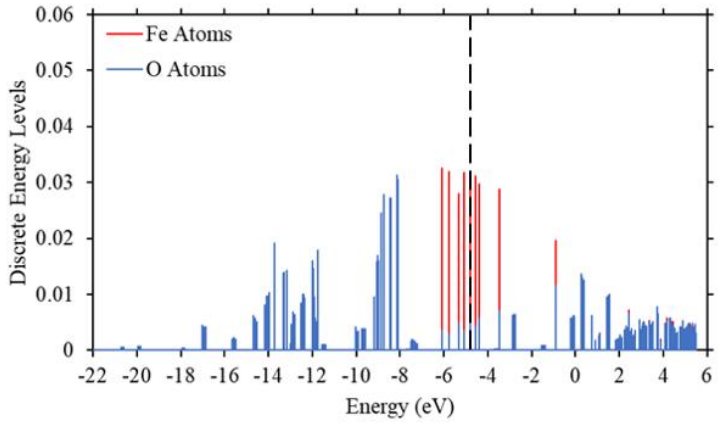

Figure S14. A. TDOS and PDOS graph of the contributions of the iron and oxygen in Fe-MOF-5-NO_2 in hexane (Trial 5). B. The discrete energy levels of the oxygen atoms (blue) and the iron atoms (red). The vertical dashed line in both A and B represents the HOMO energy level of the Fe-MOF-5-NO_2 system, which is at -4.786 eV. The y-axis represents the strength of the density of states and discrete energy levels and are unitless.

A. Density of States for Fe-MOF-5-NO_2 (DMSO)

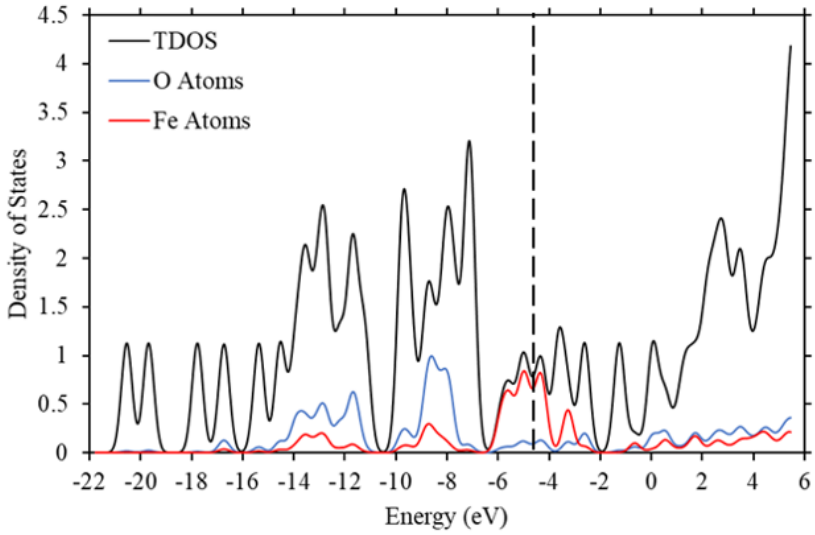

B. Discrete Energy Levels for Fe-MOF-5-NO_2 (DMSO)

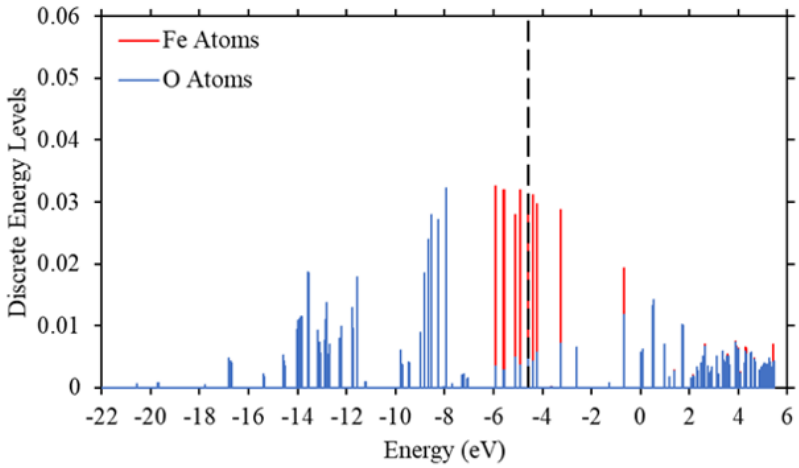

Figure S15. A. TDOS and PDOS graph of the contributions of the iron and oxygen in Fe-MOF-5-NO_2 in DMSO (Trial 10). B. The discrete energy levels of the oxygen atoms (blue) and the iron atoms (red). The vertical dashed line in both A and B represents the HOMO energy level of the Fe-MOF-5-NO_2 system, which is at -4.597 eV. The y-axis represents the strength of the density of states and discrete energy levels and are unitless.

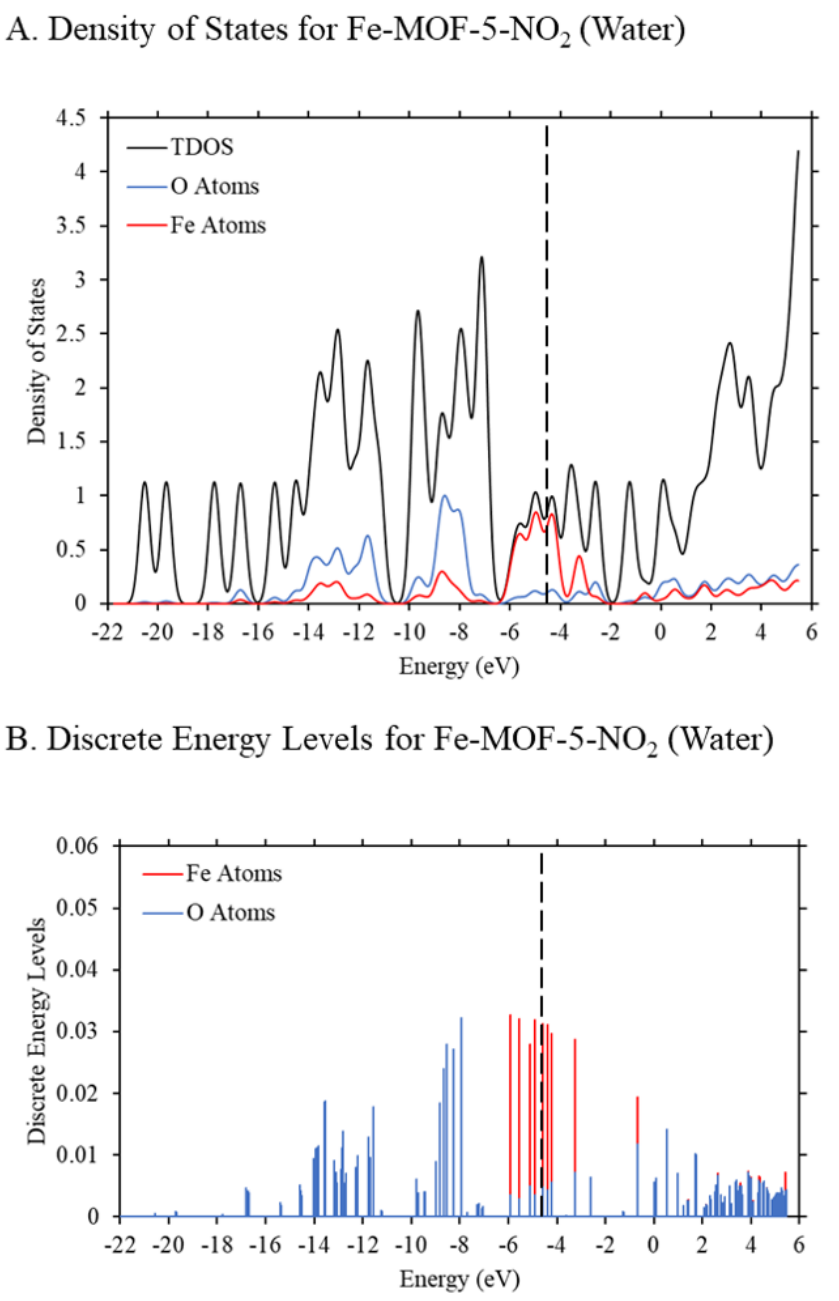

Figure S16. A. TDOS and PDOS graph of the contributions of the iron and oxygen in Fe-MOF-5-NO_2 in water (Trial 4). B. The discrete energy levels of the oxygen atoms (blue) and the iron atoms (red). The vertical dashed line in both A and B represents the HOMO energy level of the Fe-MOF-5-NO_2 system, which is at -4.594 eV . The y-axis represents the strength of the density of states and discrete energy levels and are unitless.

References

(1) ECHIP (Computer Software). Wilmington, DE: Experimentation By Design LLC; Retrieved from Http://Www.Experimentationbydesign.Com.

(2) Li, S.; Luo, P.; Wu, H.; Wei, C.; Hu, Y.; Qiu, G. Strategies for Improving the Performance and Application of MOFs Photocatalysts. *ChemCatChem* **2019**, *11* (13), 2978–2993. https://doi.org/10.1002/cctc.201900199.

(3) Tahir, M.; Ajiwokewu, B.; Bankole, A. A.; Ismail, O.; Al-Amodi, H.; Kumar, N. MOF Based Composites with Engineering Aspects and Morphological Developments for Photocatalytic CO2 Reduction and Hydrogen Production: A Comprehensive Review. *Journal of Environmental Chemical Engineering* **2023**, *11* (2), 109408. https://doi.org/10.1016/j.jece.2023.109408.